An Algorithm for Detecting Heavy-Truck Driver Fatigue from Steering Wheel Motion

David J. King
David K. Mumford
MacInnis Engineering Associates Ltd.
Gunter P. Siegmund
Canada
Paper Number 98-S4-O-10

ABSTRACT

This paper is the culmination of previous work to determine if steering behavior could be used to unobtrusively detect driver fatigue. The driving performance of 17 sleep-deprived heavy-truck drivers was monitored on a closed track. Functions in the time, frequency, and phase domains were developed to quantify changes in steering wheel input. The steering-based weighting functions which correlated most strongly with independent measures of driver fatigue and drowsiness were used to develop a simple algorithm. The algorithm predicted fatigue for all 17 volunteer drivers before the end of their test. The algorithm identified 12 drivers before a lane breach occurred, and only two drivers were not captured until a lane breach greater than 15 cm occurred. These data and the algorithm demonstrate the potential for a steering-based fatigue detection algorithm.

INTRODUCTION

Truck driver fatigue is more prevalent than either alcohol or drugs in fatal accidents (1). Therefore, being able to detect driver performance impairment in a non-invasive manner is desirable.

The driving performance of 17 sleep-deprived long-haul truck drivers was monitored on a closed-circuit track to determine whether changes in the drivers' control inputs or in the vehicle motion could be used to predict driver impairment due to fatigue. Steering measures which correlate well with driver fatigue have been previously identified (2,3). Measures of lane maintenance also correlated to driver fatigue, but not as strongly as steering-based measures.

An algorithm based on three functions derived from the steering wheel motion was developed to detect driver fatigue. A detailed explanation of this algorithm is presented and absolute limits for the cutoff values of the three functions in this algorithm are proposed.

METHODS

Test Description

A detailed description of the test configuration and instrumentation has been published (4). The test vehicle was a 1994 Freightliner conventional-cab tractor. The tractor was fitted with a short flatbed loaded with 5400 kg to improve ride-ability. The driver was instructed to maintain a constant following distance around a triangular track behind a 1992 Ford Aerostar pace vehicle. The 42 km/h test speed was maintained using the Ford's cruise control. The triangular 2.9 km track consisted of three "legs": 865, 535, and 565 metres long, respectively. Drivers attended an orientation day drive prior to reporting for their night test.

The following parameters were measured for each driver:

- vehicle speed and distance,
- steering wheel angle (θ) and angular velocity (ω),
- accelerator pedal angle and angular velocity,
- 20-lead electroencephalogram (EEG),
- heart rate (EKG),
- video of driver's face,
- vehicle lane position (using Global Positioning System [GPS]), and
- pace-vehicle following distance.

The drivers were required to remain awake for the night preceding their test. Each test began at about 11:00 p.m. and continued until either safety was compromised or the driver fell asleep. The night drives typically lasted between 2 and 3.5 hours. The safety observer intervened in three night sessions: two drivers failed to negotiate a corner in the test track; the third driver veered out of the lane toward test equipment.

Test Subjects

Seventeen volunteer male drivers completed the testing. The drivers are referred to as Drivers 1 through 19 (Drivers 5 and 17 dropped out). Table 1 lists the driver number, test duration, number of legs (straight sections completed), number of hours of sleep obtained in the preceding 24 hours, the total number of hours of sleep obtained in the preceding 48 hours, the length of an average night's sleep, and the percentage of average sleep obtained during the previous two nights. Drivers were asked not to sleep the night before the test, and therefore the ideal driver would have 50% of his normal sleep in the preceding 48 hours.

The night drives of Drivers 2, 9, and 12 were interrupted by planes landing at the airport used for the testing. This required that the safety observer communicate with the driver and the truck be stopped. The data acquired during these interruptions were discarded and the lap (consisting of 3 legs) of data surrounding the interruption was also discarded. Driver 6's night session was interrupted twice by electrical malfunction. Only the data acquired after the second interruption were used for analysis. The safety observer had to intervene for Drivers 2, 8 and 15.

Variables

Five independent variables were used to measure driver fatigue: Electroencephalography (EEG) activity in the theta band, EEG activity in the alpha band, heart interbeat interval, standard deviation of the heart interbeat interval, and subjective evaluation of drowsiness (SED) from the video data (5). Although eye blink rate can also be used to assess driver fatigue, it could not be reliably determined from the EEG or video data acquired in this study. Dependent variables in this study were steering wheel and accelerator pedal position and motion, the test vehicle speed variation, lane maintenance and car-following distance. Based on the results of previous work (2,3), only steering wheel data were used to develop the fatigue detection algorithm. Lane maintenance data were used for further evaluation.

Table 1.
Driver Information (2)

Driver Number	Total Test Duration (hr:min)	Actual Driving Time (hr:min)	Number of Legs	Sleep Acquired in Previous: 24 hrs	48 hrs	Usual Night's Sleep (hr)	Percent of Night's Sleep (24 hr avg)	Percent of Night's Sleep (48 hr avg)
1	2:47	2:17	99	0.5	3	8	6	19
2	2:27	1:51	78	0	8	8	0	50
3	2:59	2:24	102	4	10	6.25	64	80
4	3:47	3:38	144	0	8	8	0	50
6	1:24	0:55	39	0	6	6	0	50
7	4:11	3:39	156	2	9	7	28	64
8	2:14	1:43	75	0	5.5	6	0	46
9	2:44	2:13	93	4	11	6.5	62	85
10	2:45	2:11	93	2	9.5	7.25	27	66
11	3:16	2:45	120	5	9.33	7.5	66	62
12	2:48	2:17	96	1.5	4.5	7	21	32
13	3:23	2:51	120	5.5	12.5	6.5	85	96
14	3:47	3:14	135	3	10.5	6	50	88
15	1:26	0:50	35	1	6	8	13	38
16	2:24	1:49	69	4.3	11.8	6.5	67	91
18	3:17	2:44	117	2	9*	7	29	64*
19	3:06	2:31	108	3	8	6	50	67

* = Estimated Value

Scoring Steering Performance

Steering wheel position was analyzed in the time, frequency and phase domains. Scoring functions were devised in each domain to quantify different types of steering behavior.

Time-Based Functions - From the graph of steering wheel angle versus time (Figure 1) or steering wheel angular velocity versus time, differences in the steering performance early and late in the tests were evident. For instance, larger and longer duration deviations from the mean steering angle were noted as the test proceeded. Some sudden and rapid movements of the steering wheel were noted which may have been corrections after periods of inattention. Weighting functions that quantified these observations were constructed.

Frequency-Based Functions – Power spectra were calculated for the steering wheel angle and angular velocity data for each leg of a driver's test (Figures 2 and 3). Increases in the proportion of power in the lower frequencies (0 to 0.5 Hz) were noted in local areas (over 2 or more legs) and weighting functions were devised to quantify this transient behavior.

Phase-Based Functions - Phase plots of steering wheel angle (θ) versus steering wheel angular velocity (ω) were constructed (Figure 4). These plots simultaneously showed the position of the steering wheel relative to the mean and the direction in which the steering wheel was being moved. The phase plots of all drivers varied over the course of the test. Data clustered around the origin indicated a short feedback control loop and it was hypothesized that this behavior indicated an alert driver.

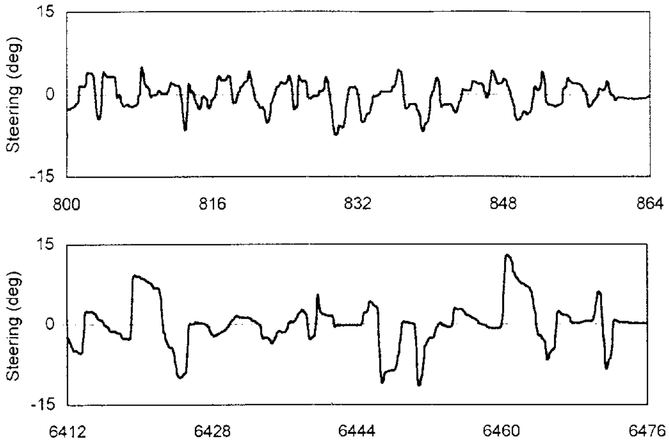

Figure 1. Early and late steering behavior in the time domain for Driver 8 (3).

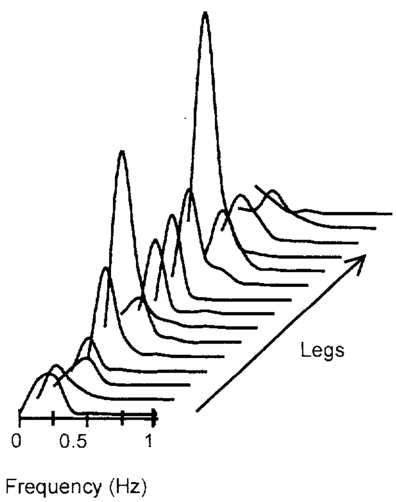

Figure 2. Variations in the power spectrum of steering wheel angle for Driver 6 (3).

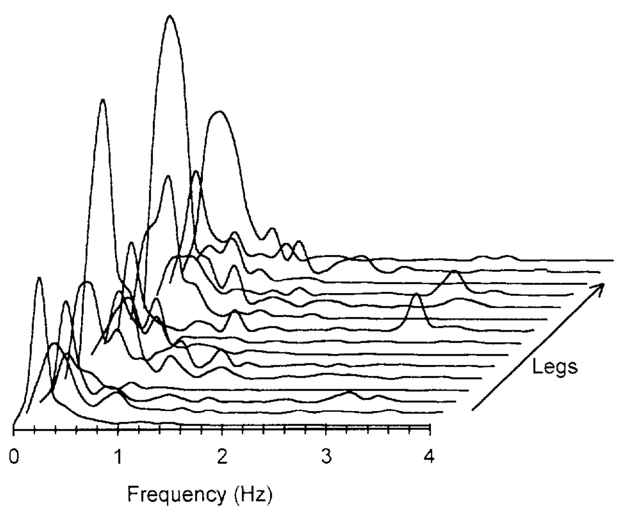

Figure 3. Variations in the power spectrum of steering wheel angular velocity for Driver 6 (3).

Loose loops, occasionally straying far from the origin, indicated longer-duration feedback, and also indicated that the driver was relying on larger and coarser steering wheel movements to control his vehicle. It was hypothesized that this behavior indicated the driver was fatigued. Small sub-clusters on the horizontal axis away from the origin (large steering angle but no angular velocity) were indicative of cornering and were particularly inappropriate on straight legs. A sample of this behavior can be seen between +5 and +10 degrees on the θ-axis of the Late Night phase plot in Figure 4. Weighting functions that quantified and penalized loose loops and small sub-clusters on the θ-axis were developed.

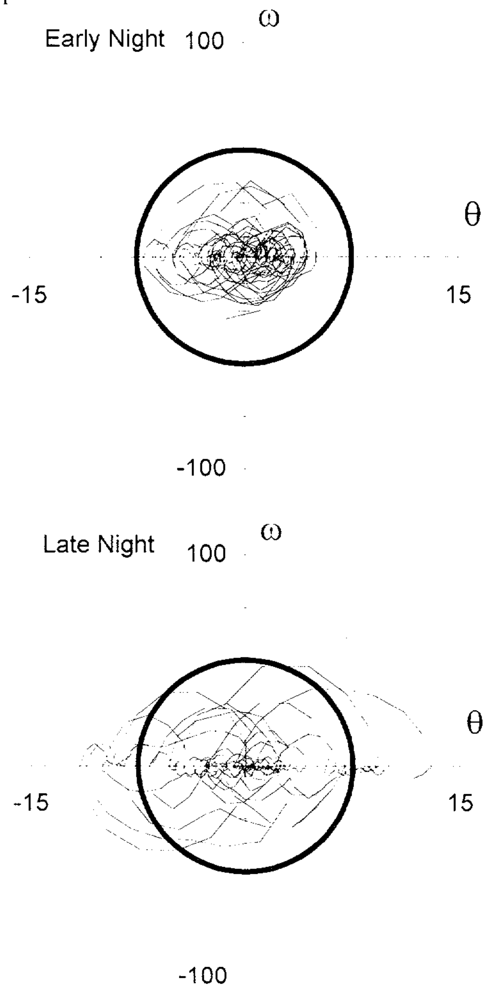

Figure 4. Sample Phase Plots from Driver 8 Showing Steering Behavior and Control Ellipse of $-7.5 \leq \theta \leq 7.5°$ and $-50 \leq \omega \leq 50$ °/s.

A subset of the phase-based weighting functions made use of a control ellipse. It was hypothesized that there was an area of the phase plot surrounding the origin in which alert drivers remained. Based on the phase plot shape of a number of early night legs from a number of drivers, a preliminary ellipse shape was chosen with a horizontal axis (steer angle, θ) of 15 degrees (from -7.5° to +7.5°) and vertical axis (steer angular velocity, ω) of 100 degrees/second (from -50 °/s to +50 °/s). Weighting functions that incorporated only portions of the phase plot outside the acceptable control ellipse were devised.

ALGORITHM DEVELOPMENT

As reported earlier (6), SED is a comprehensive measure of driver fatigue. SED was therefore used as the reference in the development of an algorithm to determine when a driver became fatigued.

To identify which weighting functions correlated best with fatigue, the coefficient of determination (r^2) between the rank order (Spearman) of each weighting function and SED was calculated. The mean r^2 across all drivers was then calculated. A minimum useful coefficient of determination was arbitrarily set to 0.5. As determined previously, ten weighting functions met this criterion (3). Of the ten, three functions were selected for the algorithm: Amp_D2_Theta, Wt Flat 0, and Outside (%) (Appendix A). The former two functions were selected because they correlated most strongly with SED. These two functions represented time-based and phase-based (control ellipse independent) measures. Of 7 phase-based measures which relied on the control ellipse, Outside (%) was selected because it correlated well with drivers who did not correlate well with the first two functions. Together, these three functions correlated with 15 of the 17 drivers. Only Drivers 3 and 4 did not correlate with these or any other functions.

The 6-leg averaged value of the three functions was calculated simultaneously from the fourth leg of each driver's test (the results from the first three legs were ignored). A simple algorithm that monitored the value of these three functions until one exceeded a specific value was used. These specific values (termed the cutoff limits) were determined by independently plotting the average SED value of all drivers over a range of possible cutoff limits (Figure 5). To select cutoff limits for each function, some level of fatigue must be used as a threshold above which a driver is deemed to be too tired to drive. The setting of this threshold level is outside the scope of this study. In order to develop a working algorithm, a SED range between 80 and 100 was arbitrarily used as the threshold above which a driver was too tired to continue driving. A SED score of 80 represents a "Moderately Drowsy" level and a score of 100 represents the level halfway between "Moderately Drowsy" and "Very Drowsy" on the SED continuum (6).

RESULTS

Based on SED levels of 80 to 100, cutoff limits (Table 2) for each weighting function were determined from the graphs in Figure 5. The lower end of the ranges in Table 2 resulted from the inclusion of all drivers and a SED cutoff level of 80.

Four drivers (3, 8, 13, and 15) were found to significantly alter the average SED and a similar series of graphs excluding these drivers was also examined (Figure 5). Three of these four drivers (3, 8, and 15) reached the maximum SED level ("Extremely Drowsy") within 30 legs (10 laps) of the start of the test. Both Drivers 3 and 15 reached a SED level of 100 within 10 legs of the start of the test. Driver 8 reached a SED level of 100 about 22 legs into his test, and fell asleep on leg 75.

For drivers 3, 8, and 15, the steering-based weighting functions lagged the rise in SED. Because of this lag and the rapid rise in SED, the three weighting functions did not reach their cutoff limits until maximum SED had been reached. It was hypothesized that in the real world the transition to "Extremely Drowsy" would not often occur this rapidly and therefore weighting-function cutoff limits excluding these data were also examined.

Table 2.
Proposed Cutoffs for Steering-Based Functions

Weighting Function	Outside (%)	Wt Flat 0	Amp_D2_ Theta
Cutoff Limits	3.1 – 10.3 (3.1 – 6)	11.2 - 16.0	5.0 - 6.3

The upper cutoff limits in Table 2 resulted from the exclusion of Drivers 3, 8, 13, and 15 and a SED cutoff level of 100.

Both the upper limits and lower limits of the ranges proposed in Table 2 were applied to the present data set of 17 drivers. The results are given in Appendix B. The upper limit of Outside (%) was assessed in greater detail, due to the relatively flat slope between SED values of 80 and 100 (Figure 5). An SED value of 100 corresponded to a Outside (%) value of 10, whereas a SED value of 93 corresponded to an Outside (%) value of about 6. Using an upper limit of 10 for Outside (%), only two drivers were captured (2 and 11). Decreasing the upper cutoff limit to 6 resulted in nine drivers being captured (1, 2, 3, 6, 9, 11, 12, 15 and 18).

Table 3 shows the average, minimum and maximum SED levels across all drivers for the upper and lower bounds of the proposed cutoff limits. Using the lower cutoff limits, all but four drivers were trapped before their SED level reached 100 ("Moderately to Very Drowsy"). Five drivers were caught before their SED level reached 40 ("Slightly Drowsy").

Table 3.
SED at Cutoff Limits

Cutoff Limits	Average SED
Lower	68 (12 - 127)
Upper	96 (39 - 152)

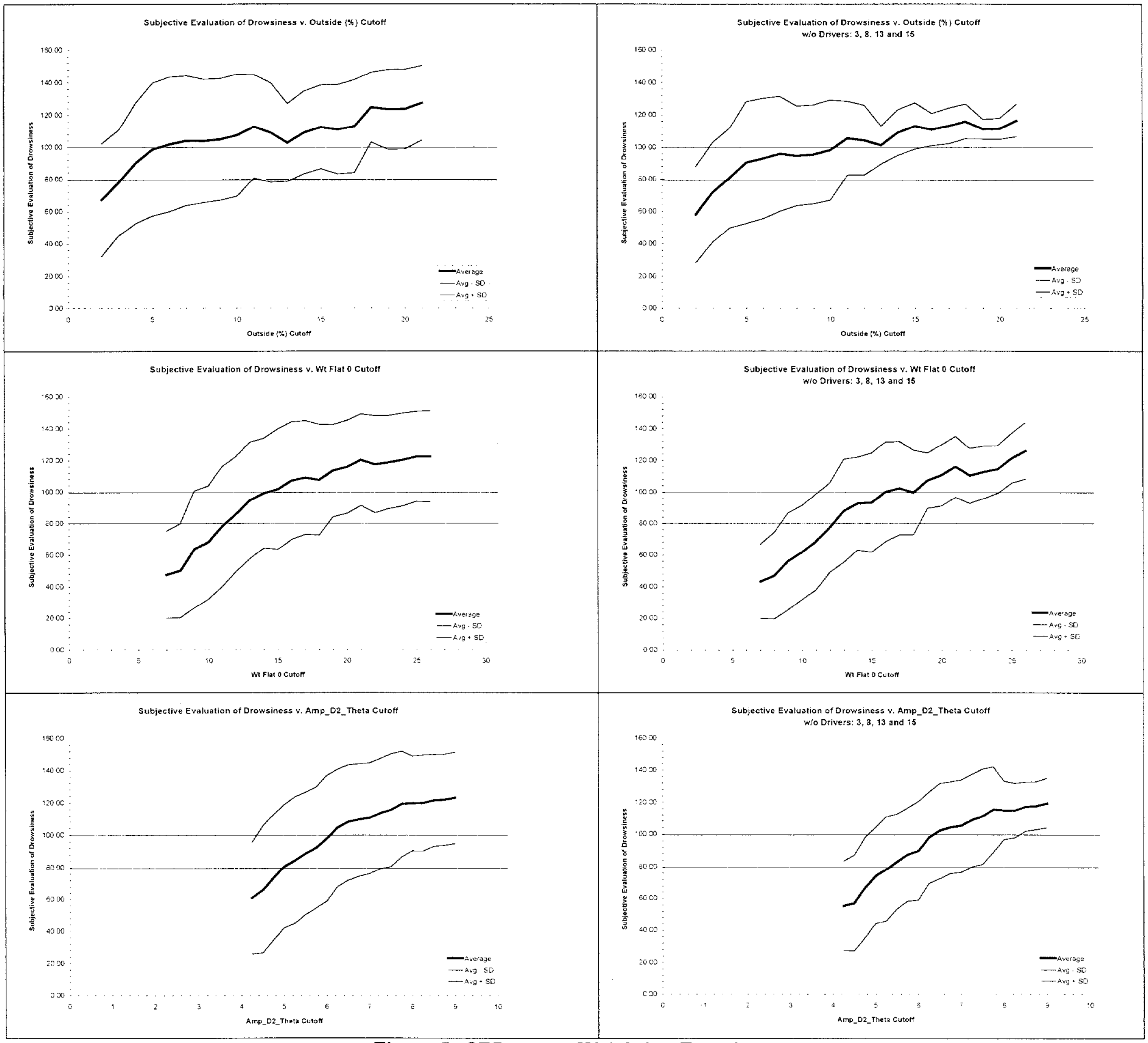

Figure 5. SED versus Weighting Functions.

Using the upper cutoff limits, eight drivers reached a SED level greater than 100, three of which were at about 150 when trapped. Only one driver was trapped before his SED level reached 40, but six were trapped before their SED level reached 80 ("Moderately Drowsy").

A comparison of the algorithm-predicted cutoff points with the lane breach data is shown in Figure 6. The horizontal axis of Figure 6, labeled "Legs", is the number of 6-leg averages. For instance, leg 20 on the horizontal axis corresponds to the average of legs 20 through 25.

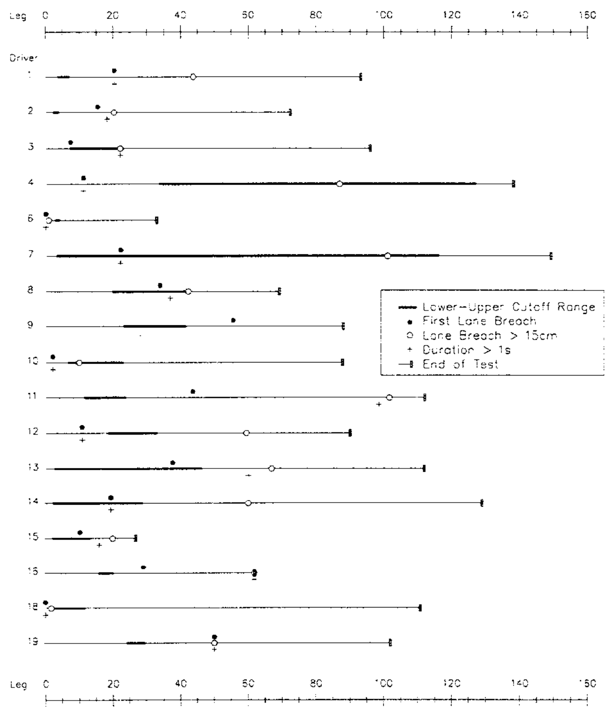

Figure 6. Summary of Algorithm and Lane Breach Cutoff Legs.

In Figure 6, the thin horizontal line terminated by the vertical mark represents the total number of 6-leg averages for each driver. This value is 5 less than the number of legs shown in Table 1 because of the effect of averaging 6 legs. The thicker portion of the line represents the range of cutoff points predicted by the algorithm using the lower and upper cutoff limits in Table 2. The lower cutoff limit corresponds to the left end of the thick line and the upper cutoff limit corresponds to the right end of the thick line.

The three symbols (•, o, and +) depict the points when the first lane breach occurred (•), the first lane breach greater than 15 cm occurred (o), and the first lane breach greater than 1 second in duration occurred (+). If a symbol is absent, then a lane breach meeting its criterion did not occur. To minimize the effect of corner-induced lane breaches, only lane breaches more than 4 seconds from the corner are shown. The relative position of the lane breach data to the thick horizontal line for each driver shows the effectiveness of the algorithm and cutoff limits.

DISCUSSION

The current algorithm and cutoff limits show that a fatigue detection algorithm based on steering wheel motion can be constructed. The algorithm trapped all 17 drivers before the end of their night drive. Figure 6 shows that for twelve of the 17 drivers, the algorithm predicted driver fatigue before or at the same time as the first lane breach occurred. For the remaining five drivers, the first lane breach and the first lane breach greater than 1 second occurred before the lower cutoff limit of the algorithm detected driver fatigue. For three of these five drivers (4, 7, and 10), the algorithm predicted fatigue before a lane breach greater than 15 cm occurred. Also, for three others among the same five drivers (6, 10, and 18), the lower limit of the algorithm detected fatigue within 5 legs of the first lane breach, i.e., within the period of the running average interval.

In only two of the five late-detection cases did a lane breach precede detection by more than 5 legs (Drivers 4 and 12). For both drivers however, the algorithm predicted fatigue before their first lane breach greater than 15 cm. Further examination of Driver 4's lane breach data indicated that his next lane breach (after the one shown at Leg 12) occurred at Leg 56 on this graph - above the lower cutoff limit of the algorithm. Driver 12's next lane breach, on the other hand, occurred at Leg 12 on this graph - still about 8 legs below the lower cutoff limit of the algorithm.

Only two drivers (6 and 18) were not captured by the algorithm before a lane breach of 15 cm. In both cases, the algorithm detected fatigue within five legs of the start of the test and within two legs of the breach. The algorithm failure for Driver 6 may be related to his initial elevated level of drowsiness. His test was interrupted twice by electrical failures and the start of his driving data was preceded by about one hour of lost data.

Driver 18's early lane breaches were a result of extended pre-corner maneuvers (he breached the lane for 8 seconds prior to one corner). It was not until leg 12 - near the upper end of the algorithm-predicted range - that he breached the lane at a distance from the corner.

The average driver reached the lower cutoff limit at Leg 12 and the upper cutoff limit at leg 36. Excluding Drivers 4 and 7, both of whom had long cutoff intervals, the average upper cutoff limit was reached at leg 24. If lane breach is a valid indicator of driver fatigue, then the results depicted in Figure 6 suggest that the lower cutoff limits proposed in Table 2 may be slightly high for some drivers. For other drivers, even the upper cutoff limit was low.

Driver 13 was the only driver who did not reach a SED level of 100 - his maximum SED was 91. He was the driver who received the largest portion of his normal sleep in the 48 hours preceding the test (96 percent). His gradual increase in SED may be more indicative of a real-world driver and suggests that cutoffs based on a SED between 80 and 100 are too high. This gradual increase in drowsiness of drivers not sleep-deprived should be explored further.

An optimal value for each cutoff limit has not been chosen for two reasons: first, data gathered at highway speeds with drivers who are initially alert and grow drowsy will be required to properly set the cutoff limits; and second, a decision on what level of SED constitutes a dangerous level must be addressed and resolved.

In addition, the question of absolute cutoff limits (applicable to all drivers) or relative cutoff limits (individual driver specific limits) has not been explored. To properly determine relative cutoff limits (e.g. doubling of a weighting function within a specific time interval), the alert values for the three weighting functions must be known. These data were not available for the drivers in this study.

The weighting functions and algorithms were developed from data gathered in straight leg sections with intervening corners. On average, half of each lap was spent cornering and the other half was spent on the straight sections, which means that only half of the data gathered was used. In a real world application, data would probably be gathered more continuously and the time length of the running averages may need modification. It is not known to what degree the intervening corners delayed fatigue development. Data gathered from truck drivers on the road will be required to confirm the appropriate time length for the running averages.

The cutoff values were developed from data gathered from a specific truck on a specific track under test conditions. Moreover, all of the data were gathered at a nominal speed of 42 km/h. Testing of other trucks on real roads at highway speeds must be conducted to validate the weighting functions, the algorithm, and the cutoff limits. Different steering-box ratios on other trucks may also alter the cutoff limits.

If a fatigue detection device is to be used predominantly on highways, then some means of determining that the vehicle is travelling at highway speed will be necessary. For example, the frequency of gear shifts could be monitored. Periods of high-speed travel and low gear-shifting frequency could be useful precursors to the onset of fatigue (7).

Almost all of the drivers in this study were sleep-deprived prior to starting their test. Because the drivers were not monitored from an alert condition into a fatigued condition while driving, the proposed cutoff limits may be subject to modification. Real-world testing of initially-alert drivers must be conducted to confirm or modify these cutoff limits.

Lane maintenance may be a valuable independent measure of driver fatigue as imaging technology develops and becomes more affordable. Combining lane maintenance and steering wheel data will reduce the potential for misdiagnosing driver fatigue.

In summary, three steering-based weighting functions are recommended for detecting driver fatigue: Outside (%), Wt Flat 0, and Amp_D2_Theta. The proposed absolute cutoff limits for the three weighting functions are shown in Table 2. These proposed cutoff limits were based on SED levels of 80 and 100, and on data acquired under controlled conditions. They are necessarily preliminary and are subject to confirmation by on-the-road testing. The proposed algorithm captured all 17 drivers before the end of their night test. Twelve of the drivers were detected before any lane breaches occurred. Only two drivers were not captured before a lane breach greater than 15 cm occurred, and both of these drivers were captured within two legs of this lane breach.

ACKNOWLEDGMENTS

The data for this paper were collected for a fatigued driver identification study for the Insurance Corporation of British Columbia (ICBC). The authors would like to thank ICBC for permitting the publication of these findings.

REFERENCES

1. Knipling, RA., and Wang, J-S, "Crashes and Fatalities Related to Driver Drowsiness/Fatigue", Research note, Washington, DC, U.S. Department of Transportation, NHTSA, 1994.
2. Siegmund, GP, King, DJ, and Mumford, DK, "Correlation of Heavy-Truck Driver Fatigue with Vehicle-Based Control Measures", SAE 952594, 1995.
3. Siegmund, GP, King, DJ, and Mumford, DK, "Correlation of Steering Behavior with Heavy-Truck Driver Fatigue", SAE 961683, 1996.
4. King, DJ, Siegmund, GP and Montgomery, DT, "Outfitting a Freightliner Tractor for Measuring Driver Fatigue and Vehicle Kinematics During Closed-Track Testing", SAE 942326, 1994.
5. Ellsworth, LA, Wreggit, SS, and Wierwille, WW, "Research on Vehicle-Based Driver Status/Performance Monitoring"; Third Semi-Annual Research Report, Sept. 92 to Mar 93. Dept. of Industrial and Systems Engineering, Report No. 93-02, Blacksburg Virginia: Virginia Polytechnic Institute and State University; 1993.
6. Wierwille WW and Ellsworth LA. "Evaluation of Driver Drowsiness by Trained Raters", Accident Analysis and Prevention, Vol. 26, No. 5, pp. 571-581, 1994.
7. Yamamoto K, Hirata Y, and Higuchi S, "Estimate of Driver's Alertness Level Using Fuzzy Method", SAE 942321, 1994.

APPENDIX A - STEERING-BASED WEIGHTING FUNCTION FORMULAE

Various weighting functions based on steering angle (θ), steering angular velocity (ω), and combinations of the two were developed. Three ways of viewing the data were used to develop the weighting functions:

Time-based: weighting functions developed from variations in θ or ω plotted against time,

Frequency-based: weighting functions developed from variations in the power spectrum,

Phase-based: weighting functions developed from variations in θ plotted against ω (no time dependence).

The three weighting functions referred to in this paper are outlined below:

Time-Based Weighting Functions

Both θ and ω were plotted against time and weighting functions were devised to score variations present in these variables as the driver tired. As discussed, Amp_D2_Theta was selected for determining a cutoff point:

Amplitude Duration Squared Theta - (*Amp_D2_Theta*) - Each distinct area between theta and the mean of theta over the length of one leg was multiplied by the length of time the steering angle remained on that side of the mean. The area under the θ-curve was calculated using trapezoidal integration. Figure A1 shows the variables used to calculate Amp_D2_Theta.

$$Amp\_D2\_Theta = \frac{100}{N}\sum_{j=1}^{J}\left(A_j^{\theta} t_j^{\theta}\right) \quad \text{(A1)}$$

where A^{θ}_j = the jth area block in the (θ-θ_m) data of the leg,
t^{θ}_j = the length of the jth area block in the leg,
J = the total number of area blocks in the leg,
= Z+1 (see Zero Crossings below),
N = total number of samples in leg, and
100 is a scaling factor.

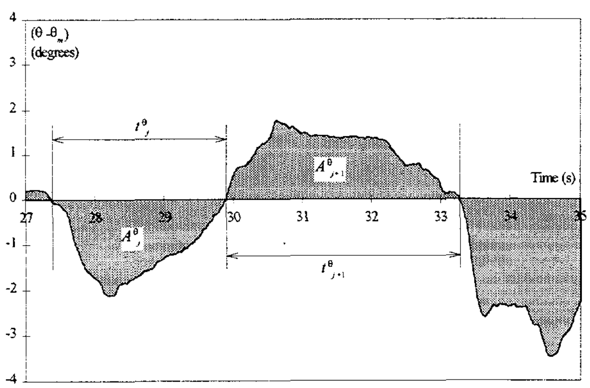

Figure A1. Definition of variables for calculating Amp_D2_Theta.

Phase-Based Weighting Functions

Phase-based weighting functions were developed by examining the phase plot of steering angle (θ) versus steering angular velocity (ω) (see Figure A2). These functions were broken into two sub-groups: functions dependent on a hypothesized control ellipse, and functions independent of the control ellipse.

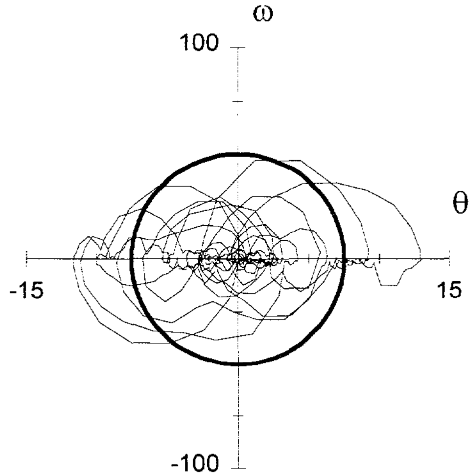

Figure A2. Example of Phase Plot with Control Ellipse.

Ellipse-Dependent Weighting Functions

A control ellipse with a horizontal (θ) axis length of $2a$ and a vertical (ω) axis length of $2b$ was superimposed onto the phase plot of θ versus ω. Steering behavior outside the control ellipse was penalized, whereas steering behavior inside the ellipse was considered normal. Different ellipse dimensions (a,b) were also investigated: a was varied between 3° and 9° in 1.5° increments, and b was varied between 20°/s and 60°/s in 10°/s increments. Values of ±7.5° and ±50°/s were selected.

Outside (%) - (*Outside*) - The percentage of (θ,ω) points per leg outside the control ellipse including single point episodes.

$$Outside = 100\frac{n}{N} \quad \text{(A2)}$$

where n = number of points outside control ellipse,
N = total number of sampled points in leg, and
100 is a scaling factor.

Ellipse-Independent Weighting Functions

Weight Flat Zero - (*Wt Flat 0*) – only (θ_i,ω_i) points in the phase space satisfying the condition $|\omega| \leq \omega_c$ with ω_c = 5 °/s are included in the calculation. All points satisfying this condition are weighted by the square of the distance from the origin.

$$Wt.\ Flat\ 0 = \frac{100}{N}\sum_{i=1}^{N}\left(\frac{(\theta_i - \theta_m)^2}{a^2} + \frac{\omega_i^2}{b^2}\right) \quad \text{(A3)}$$

only for $|\omega_i| \leq \omega_c$

where θ_i = ith value of the steer angle,
θ_m= mean value of all θ's for leg,
a = half axis length of ellipse in θ dimension,
ω_i = ith value of steer angular velocity,
ω_c = cutoff value of omega (5 °/s),
N = total number of sampled points in leg, and
100 is a scaling factor.

APPENDIX B – ALGORITHM PERFORMANCE

Two tables are presented, showing the results of running the algorithm through the current set of 17 drivers using first the lower cutoff limits (Table B1) and then the upper cutoff limits (Table B2).

ALGORITHM RESULTS

Table B1 Cutoff results for all Drivers using a SED value of 80

		Driver Number																			
	Limit	1	2	3	4	6	7	8	9	10	11	12	13	14	15	16	18	19	Min	Avg	Max
Total legs driven		99	78	102	144	39	156	75	93	93	120	96	120	135	35	69	117	108	35	99	156
Cutoff Leg		4	3	8	35	3	3	21	23	7	12	20	3	3	4	18	3	27	3	12	35
Leg where SED = 80		17	16	1	74	2	128	10	30	3	21	21	106	47	2	15	88	28	1	36	128
SED at cutoff		39	54	122	67	86	18	127	69	109	60	79	12	35	92	103	19	75	12	68	127
Maximum SED for all legs		124	150	157	132	135	103	160	135	141	154	153	91	137	160	155	151	154	91	141	160
Maximum SED before capture		39	54	122	73	86	18	127	69	109	60	79	12	35	92	103	19	75	12	69	127
Outside (%)	3.1	3.93	6.06	3.34	1.61	8.99	0.85	3.01	3.72	2.36	3.70	3.20	0.63	3.89	3.22	1.23	2.30	2.36	0.63	3.20	8.99
Wt Flat 0	11.2	9.4	10.7	13.1	9.7	16.2	8.1	10.1	8.9	8.6	10.9	11.3	8.3	10.3	10.6	9.6	11.7	10.9	8.1	10.5	16.2
Amp_D2_Theta	5	4.72	4.6	5.8	5.1	6.27	5.49	5.49	3.71	5.11	3.28	3.83	5.04	3.92	3.36	5.1	4.34	5.22	3.28	4.73	6.27

Table B2

Cutoff results for all Drivers using a SED value of 100

		Driver Number																			
	Limit	1	2	3	4	6	7	8	9	10	11	12	13	14	15	16	18	19	Min	Avg	Max
Total legs driven		99	78	102	144	39	156	75	93	93	120	96	120	135	35	69	117	108	35	98.8	156
Cutoff Leg		7	3	24	128	3	117	44	40	23	24	34	47	30	15	22	12	32	3	35.6	128
Leg where SED = 100		23	21	4	102	7	143	14	51	6	46	28	999	73	6	18	94	32	4	98	999
SED at cutoff		44	54	151	123	86	68	153	95	131	89	116	43	70	149	123	38	101	38	96	153
Maximum SED for all legs		124	150	157	132	135	103	160	135	141	154	153	91	137	160	155	151	154	91	141	160
Maximum SED before capture		44	54	151	132	86	69	158	95	131	89	116	43	70	149	123	38	101	38	97	158
Outside (%)	6	6.82	6.06	6.18	3.78	8.99	1.29	4.22	6.24	3.18	6.19	6.13	2.18	5.15	8.42	4.86	6.37	4.47	1.29	5.33	8.99
Wt Flat 0	16	13.6	10.7	13.8	14.4	16.2	8.5	13.6	14.4	13.1	12.3	13.4	12.4	16.4	17.9	14.9	15.4	15.3	8.5	13.9	17.9
Amp_D2_Theta	6.3	6.57	4.60	6.85	7.95	6.27	6.45	7.03	5.80	6.59	4.15	4.69	6.30	5.29	6.01	6.34	5.31	6.62	4.15	6.05	7.95